Adsorption Characteristics of Cobalt and Nickel on Oxalate-Treated Activated Carbons in Sulphate Media

Henry Kasaini, Paul Thabo Kekana, Amirali Alizadeh Saghti, and Kim Bolton

Abstract**—**This paper presents adsorption results concerning cobalt and nickel ions on the surface of activated carbons (ACs) functionalized by oxalate ions ($KC_2O_4^-$, $C_2O_4^{2-}$). The parameters which tend to favour the adsorption of oxalates were optimized and the surface morphology of the modified ACs were determined by means of Scanning Electron Microscopy (SEM) while the evidence of anchored oxalate groups was highlighted by Fourier transform infrared spectroscopy (FTIR) measurements. These experimental studies were complemented by computer simulations to investigate the capacity of AC surface groups (carboxylic, esters, ethers and ketones) to bind with oxalate molecules in acidic solutions. Results showed that under neutral conditions the oxalate ($C_2O_4^{2-}$) prefers to attach to carboxylic acid groups on the AC surface. The experimental parameters investigated include initial solution pH, metal concentration, adsorbent dose and temperature. The maximum uptake of Ni(II) and Co(II) by the oxalate-modified ACs were 52.63mg/g and 50.76mg/g, respectively.

Keywords**—**Activated Carbons, Adsorbent, FTIR, Isotherms, Kinetics, Potassium oxalate.

I. Introduction

ACTIVATED carbons (ACs) are effective adsorbents for a wide variety of organic and inorganic pollutants found in industrial effluents. The large adsorption capacity of ACs is attributed to a high pore volume and large surface unit area as well as the presence of a wide spectrum of surface functional groups [5], [1]. The low cost of ACs and simplicity of activation procedures make the application of carbon adsorbents attractive especially with regards to adsorption of toxic heavy metals [34].

In the past decade, several publications have appeared demonstrating the ability of ACs to anchor functional molecular groups such as amines [17]-[19] for the purpose of selective extraction of precious metals from mixed solutions.

There is scanty literature about functionalization of ACs with oxalate compounds in order to beneficiate metals from acidic solutions.

Henry Kasaini is with Rare Element Resources Ltd, Lakewood 80228. Denver Area, Colorado, USA. (e-mail:henry_kasaini@yahoo.com)

Paul Thabo Kekana is with Tshwane University of Technology Department of Chemical and Metallurgical Engineering. P/BagX680,Pretoria, South Africa. (e-mail: tpkekana@yahoo.com)

Kim Bolton and Amirali Alizadeh Saghti are with School of Engineering, University of Borås, SE-501 90, Borås, Sweden.

It has been demonstrated by [15] that Ni(II) can be effectively eliminated from aqueous solution using activated carbon prepared from biomass. A maximum uptake of 54.35mg Ni(II)/g AC was obtained by the authors. Ni(II) was successfully sequestered from solution using activated carbon prepared from *Parthenium hysterophorus L* [28]. The adsorption of Ni(II) was found to be highly dependent on pH, initial metal concentration and adsorbent dose. The effect of pH on the adsorption of Ni(II), Co(II), Cd(II), Cu(II), Pb(II), Cr(II) and Cr(VI) ions from aqueous solutions by activated carbon prepared from apricot stone was investigated by [20]. The adsorbent material was activated with H SO_4 (1:1) at 200^{o}C for 24 hours. Maximum removal of Cr (VI) occurred at pH 1 and at 3-6 for other metals studied. It was demonstrated that Ni(II) could be effectively adsorbed from aqueous solutions using activated carbon prepared from coirpith [16]. The optimization of Ni(II) adsorption from aqueous solutions was successfully investigated by [8].

Numerous researchers have reported on chemical modification of ACs as a means to enhance their adsorptive capacities towards heavy metals. The presence of functional groups on the surface of the carbon matrix facilitates the attachments of various molecular groups [5]. The modification techniques of ACs can be categorized as being chemical, physical and biological in nature.

Palm shell activated carbon impregnated with polyethyleneinime was used to adsorb Cd(II) ions from solution [39]. Two polyethyleneimine polymers were used and only the low molecular weight polymer was successfully impregnated on the surface of the AC. This resulted in the enhancement of adsorption of the adsorbent towards Cd(II) ions. The adsorption of Cu(II) using AC modified with sodium acetate was studied by [27]. The modification improved the adsorption capacity of the plain activated carbon by a factor of 2.2. The adsorption of Co(II) onto bagasse pith sulphurized activated carbon was studied by [21]. The pH of zero charge for the sulphurized activated carbon was 4.3 and maximum adsorption was obtained in the pH range 4.5-8.5. The adsorption of heavy metals with activated carbon impregnated with anionic surfactants was investigated by [2]. The enhanced removal of Cd(II) by the modified adsorbent was attributed to the negatively charged groups in the hydrophilic head of anionic surfactant that interacted with the Cd(II) ions.

Techniques that are used to remove metals from solution include chemical precipitation, electro deposition, ion

exchange, membrane separation, ion exchange and activated carbon adsorption [31]. The choice of treatment depends on effluent characteristics such as the concentration of the metal ion, pH, temperature, flow volume, biological oxygen demand (BOD) and the economics involved. Adsorption is a versatile treatment technique practiced widely in fine chemical and process industries for wastewater and gas treatment. The adsorption process is simple to operate and the adsorbent can be recovered and reused [1].

Oxalate compounds are used to precipitate metal ions from solutions. For example, cobalt from lithium-ion batteries was leached and precipitated using ammonium oxalate by [36]. Nickel (98%) from a spent catalyst has been recovered by precipitation using ammonium oxalate [32]. Nickel oxalate particles were synthesized using emulsion liquid membranes with oxalic acid as the precipitating agent [40]. The quantities of oxalate chemicals used in liquid-liquid precipitation operations are very large and their exorbitant market price results in high operational costs in metallurgical plants. Therefore, there has been an attempt to replace oxalate compounds with cheaper precipitants or selective resins. There is scanty information about the immobilization of oxalates on adsorbent substrates because they are mostly used for precipitation of metals from solutions.

The objective of this study was to optimize the process of anchoring oxalate groups on the surface of ACs and to employ the oxalate- modified ACs to sequester cobalt and nickel ions from dilute industrial solutions. The test protocol commenced with optimizing the conditions at which oxalate would be strongly bound to the activated carbon pellets such as solution pH, adsorbent dose and temperature. Parameters which affect the adsorption of Co(II) and Ni(II) such as contact time, initial solution pH, initial metal concentration, adsorbent/liquid ratio and temperature were investigated. The kinetic data was fitted to the pseudo-first-order and pseudo-second-order models and the equilibrium data was fitted to the Langmuir and Freundlich isotherm models. The evidence of oxalates on the surface of ACs was developed through by FTIR and SEM measurements.

The experiments are complemented with computational studies in order to shed light on some of the most important interaction mechanisms and structures that are involved in the adsorption on the activated carbon (AC). The simulations are for simplified systems and do not, for example, take account of the changes in pH that are investigated in the experiments. Instead, they focus on the interaction of the oxalate groups with the activated carbon surface and how these interactions are affected by water medium. In particular, the structures and binding energy of oxalate ions adsorbed on non-functionalized regions of the AC as well as on carboxylic acid, ketone, ether and ester functionalized surfaces are studied. The qualitative study provides information on which of these functional groups is most important in the adsorption process at the point of zero charge of the surface.

II. Experimental

The activated carbon pellets (USA Norit) and analytical grade Potassium oxalate ($K_2C_2O_4$) were purchased from Sigma Aldrich. Stock solutions (1000mg/L) of Ni(II) and Co(II) were prepared by dissolving the required amounts of $NiSO_4$ and $CoSO_4$ in deionized water. The stock solutions were diluted with deionized water to obtain concentrations in the range 10 to 150mg/L. All the chemicals used in the study were of analytical grade.

An excess oxalate solution was prepared by dissolving potassium oxalate in deionised water until the solids could not dissolve any further. The pH of the oxalate solution was adjusted to 11 using dilute sodium hydroxide prior to the immersion of the native activated carbon. A weighed sample of the native activated carbon was immersed in the oxalate solution in a 250mL air tight plastic bottle and the bottle was placed in a shaking water bath for 18 hours. The temperature and the rotational speed of the shaking water bath were fixed at 343K and 200 rpm, respectively. After 18 hours, the oxalate solution was decanted and the activated carbon particles were washed repeatedly to remove the excess modifying agent from the surface. The washed AC particles were dried in a drying oven for 18 hours at 353K.

The adsorption of Co(II) and Ni(II) was conducted by contacting 50mL of metal solutions with predetermined amounts of adsorbent in 100mL air-tight bottles. The samples were agitated in a thermostated water bath at a speed of 200rpm to ensure adequate mixing. The initial pH of the feed solutions was adjusted by adding small amounts of dilute NaOH or H_2SO_4. At predetermined intervals, samples were drawn from the AC/liquid mixtures and immediately filtered through a centrifuge lined with a Whatman 42 filter paper. All batch experiments were carried out at different temperatures in the range 298-343K. The supernatant was analyzed for solution metals by means of atomic absorption spectrophotometry (AAS).

The initial solution pH was varied in the range 3-7 with the initial metal concentration and adsorbent dose fixed at 30 mg/L and 2g/L, respectively. The adsorption kinetic study was conducted in a period of 150 minutes. 0.2 g of adsorbent was contacted with a 50mL Ni(II)/Co(II) solution with the initial concentration and pH fixed at 50mg/L and 6, respectively. Samples were withdrawn at predetermined time intervals and immediately filtered. The initial metal concentration was varied in the range 30-150mg/L with the pH and adsorbent dose fixed at 6 and 2g/L, respectively. The adsorption period was fixed at 24 hours. Ni(II) and Co(II) solutions with an initial concentration 30mg/L and pH of 6 were contacted with adsorbent of different dosages (1-5g/L). The solutions were filtered from the adsorbent after an adsorption period of 24 hours.

The uptake of metal ions was calculated by the difference in their initial and final concentrations. The mass balance is expressed mathematically as:

$$q = \frac{V(C_o - C_e)}{M} \quad (1)$$

Where q is the amount of metal ion adsorbed per unit mass of adsorbent (mg/g adsorbent), V is the volume of the

metal solution (L), C_o is the initial concentration of metal ion in the aqueous phase (mg/L), C_e is the final concentration of metal ion in the aqueous phase (mg/L) and M is the mass of adsorbent used (g). The percentage adsorption was calculated as follows:

$$\% \, Adsorption = \frac{(C_o - C_e)}{C_o} \times 100 \quad (2)$$

III. Simulations

The AC surface was modeled as a single benzene ring (for the non-functionalized surface) or as a benzene ring with a hydrogen replaced by one the functional groups listed in the Introduction. This is the smallest system that has the electron resonance that is found in AC (and that may be important for adsorption energies and mechanisms) and has also successfully been used in previous studies of adsorption of methylamine on AC [26]. In addition, studies performed by us on the adsorption of oxalate on larger surfaces (containing 12 hexagonal rings) shows similar structures as those reported here and shows that the oxalate binds to the functional groups. (Although there is qualitative agreement between the results obtained from the larger and smaller systems, the binding to the functional group on the larger system is typically weaker than that on the smaller benzene system. This is because hydrogen atoms on the model benzene ring are closer to the oxalate ion than the hydrogen atoms on the larger surface, which increases the binding energy between the functionalized model benzene ring and the ion).

The calculations were performed using the COMPASS force field. This force field includes terms for bond stretching, angle bending, out-of-plane torsions and wags, cross-terms that couple these intramolecular motions, and intermolecular interactions that are described by electrostatic and van der Waals terms. The parameters for the intramolecular terms as well as the atomic charges have been fit to empirical data [35], and those for the intermolecular terms are fit to *ab initio* data [11]. The fit has been made to a variety of materials including polymers, metals, some metal ions, metal oxides, inorganic small molecules and most common organics [4]. In addition, this force field has been used to study the adsorption of methylamine on AC [26], and gave results that were in good agreement with first principles calculations.

The binding energies of the AC-oxalate complex were determined from

$$E_{bind} = E_{AC-oxalate} - E_{AC} - E_{oxalate} \quad (3)$$

where $E_{AC-oxalate}$ is the energy of the AC-oxalate complex. E_{AC} is the energy of the AC and $E_{oxalate}$ is the energy of the oxalate ion. All of these energies are obtained from the minimum energy structures. These structures were obtained by performing conformational searches using simulated annealing with 5 annealing cycles. During each cycle the structures are heated and cooled in 25 K ramps, with 10^4 steps per ramp. The integration step size was 1 fs which yields an annealing time of between 1.25 ns (for a mid-cycle temperature of 400 K) and 20 ns (for a mid-cycle temperature of 800 K).

The annealing was performed in the isothermal (NVT) ensemble during each ramp, where the temperature of the initial (and final) ramp of each cycle was 300 K and the mid-cycle temperature was varied between 400 and 800 K (i.e., typically five annealing simulations with different mid-cycle temperatures were performed for each of the chemical species). The minimum energy structure is obtained at the end of each cycle using a combination of the steepest decent, conjugate gradient and Newton methods [23]. This procedure allows the energy to be minimized gradually without trapping the structure in local energy minima. Although this method does not guarantee that the global energy minimum energy structure is obtained, the fact that the vast majority (usually all) of the geometry optimizations yield the same structure is strong indication that the chemically relevant minimum energy structure was identified.

The same annealing method was used when surrounding the AC-oxalate complex with between one and six water molecules. The simulations using six water molecules typically showed that a few (usually one or two) of these water molecules formed water clusters that were not strongly attached to the complex. Addition of more water to the simulation merely increases the size of these clusters, and does not affect the structure of the complex. Hence, using six water molecules is sufficient to assess the role of the water medium on the complex structure. The structures obtained from these simulations were used to identify the preferred binding sites of the water molecules. In addition, the effect of the water on the AC-oxalate complex structure was analyzed by comparing this structure in the absence and presence of the water.

IV. Results and Discussion

A. Characterization of Adsorbent

1. Scanning Electron Micrograph (SEM)

The surface morphology of the oxalate-modified AC adsorbent was studied using a scanning electron microscope (JEOL Model JSM-5800LV). The adsorbent sample were transferred to the SEM specimen chamber and observed at an accelerating voltage of 8kV and 11 mm working distance. The SEM micrograph for the oxalate-modified carbon sample is illustrated by Fig. 1. After modification the adsorbent was covered by a layer of deposited species which resulted in the formation of an irregular surface, indicative of a high surface area.

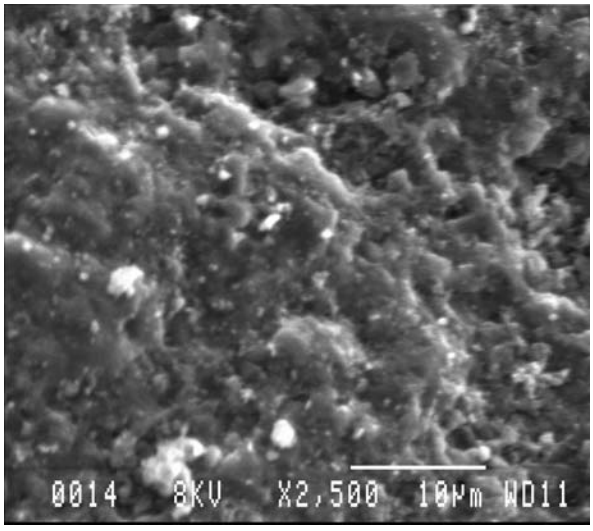

Fig. 1 Scanning electron micrograph of oxalate-modified AC

2. Surface Chemistry

The surface chemistry of the oxalate-modified carbon adsorbents was determined using Fourier transform infrared spectrophotometry (Perkin Elmer). The adsorbent particles were ground into a fine powder and dispersed in a mineral oil (Nujol). The suspension was placed between sodium chloride plates and the spectra were recorded from 800 to 4000 cm^{-1} wave number. Fig. 2 represents the spectra of the oxalate-modified carbon. From Fig. 2, the peak at 2838 cm^{-1} is assigned to the sp^3 alkane group. Peaks at 1455 and 1354 cm^{-1} are also assigned to the CH_3 groups. Peaks at 1199 and 1102 cm^{-1} are attributed to the C-O groups. Because the oxalate attaches as an anion on the AC surface, there is a resonance between the C and two O atoms and this increases the single bond character and lowers the C=O absorption frequency. The peak at 1404 cm^{-1} is assigned to the COO^- group.

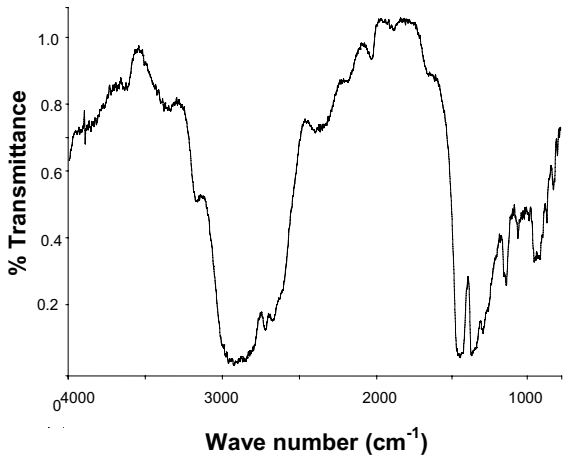

Fig. 2 FTIR spectrum of oxalate-modified AC

B. Batch Adsorption Test Results

Preparation of oxalate-modified AC adsorbents:

Activated carbon pellets (Norit 0.8, USA) were modified by being contacted with oxalate solutions which were prepared at different pH values (3, 7 and 11). Co(II) and Ni(II) were used as adsorbates to study the adsorption characteristics of ACs, which were modified at pH 3, 7 and 11. The pH values used for the modification of the ACs were not necessarily the same as those used during metal adsorption. Fig. 3 and 4 show the recovery profiles as a function of initial pH of solution for Ni (II) and Co (II) ions, respectively.

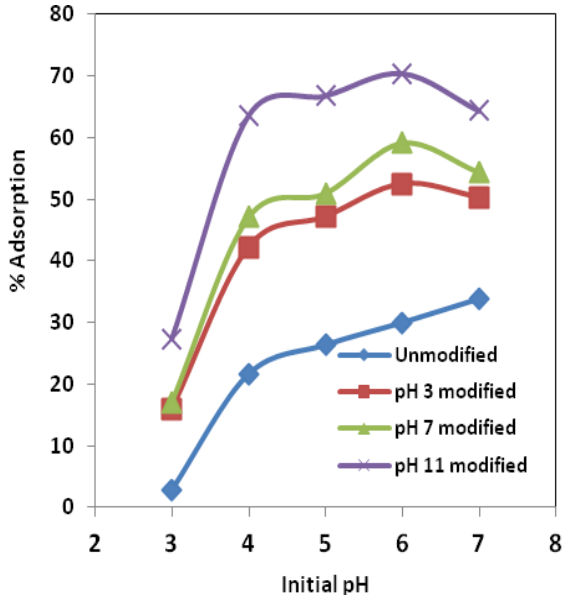

Fig. 3 Effect of pH on the extent of Ni (II) adsorption on AC modified at three different pH values

The adsorption profiles of Co(II) and Ni(II) followed the same trend but differed in the extent of adsorption. This is because both Ni (II) and Co(II) species are positively charged in low pH solutions. Covalent bonding between the negatively charged oxalate functional groups on the AC surface and the positively charged metal ions is responsible for the removal of the metal ions from solution.

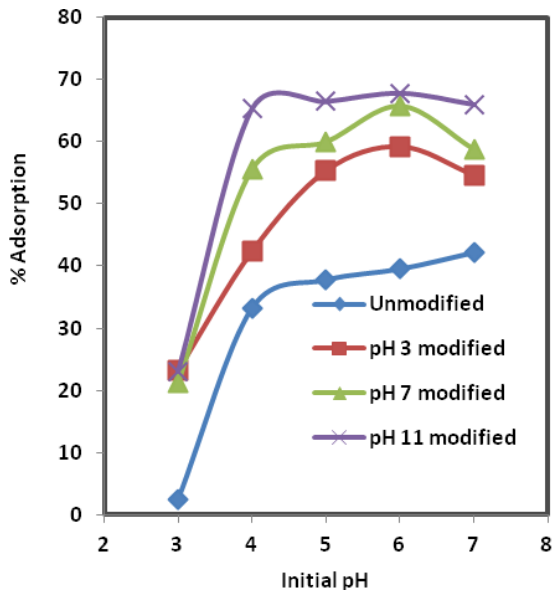

Fig. 4 Effect of pH on the extent of Co (II) adsorption on AC modified at three different pH values

The pH at which the adsorbent was modified had a profound effect of the performance of the AC adsorbents to sequester metals from solutions. The adsorptive properties of the AC adsorbents were improved compared to unmodified AC and highest extent of adsorption was observed for the AC modified at pH 11. The adsorption mechanism of the metals onto the modified adsorbent could be explained by the displacement of K^+ ions by Co(II) and Ni(II) to preferentially bind with the oxalate molecules. This is illustrated by (4) and (5). It is postulated that the entire potassium-oxalate complex is irreversibly adsorbed on the surface of ACs during the modification stage when the AC adsorbent is contacted with a solution of potassium oxalate. This is because K^+ ions diffuse to the surface of the AC and attract the oxalate anions by ionic bonding to maintain electrical neutrality on AC surface. The oxalate anions also bond with the carboxylic acid functional groups on the AC surface by covalent bonding.

$$K_2C_2O_4 + Co^{2+} \leftrightarrow CoC_2O_4 + 2K^+ \quad (4)$$

$$K_2C_2O_4 + Ni^{2+} \leftrightarrow NiC_2O_4 + 2K^+ \quad (5)$$

The speciation of potassium oxalate ($K_2C_2O_4$, $KC_2O_4^-$, $C_2O_4^{2-}$) in acid solution depends on feed solution pH. There is scanty literature on the speciation of potassium oxalates in solution and hence several tests were required to find the optimum conditions at which the uptake of oxalates by ACs was significantly high.

Adsorption performance of oxalate-modified ACs:

The adsorption behavior of oxalate-modified ACs is illustrated in Fig. 5 and 6. These tests were conducted under conditions where initial metal concentration and AC mass/liquid ratios were not optimized. The initial pH of the solution has a significant effect on the uptake of Co(II) and Ni(II) in the temperature range tested. An increase in the solution pH increased resulted in the increase in uptake of the metal ions. For Co(II) at 298K, an increase in pH from 3 to 4 resulted in a rapid increase in uptake from 4.62 to 9.80mg/g. Any further increase in pH resulted in a marginal increase in uptake until a maximum uptake of 10.57mg/g was obtained at an optimum pH of 6. Further increases in pH beyond this point resulted in a decline in uptake of the metal ions. This was as a result of precipitation of metals ions at pH values beyond 6. The same result was obtained by [41] when they used DHMP loaded activated carbon to adsorb Cu(II), Co(II), Ni(II) and Pb(II).

The increase in competition of the metal ions with protons for the adsorption sites is suggested as the reason of the low uptake of the metal ions in the acidic pH range [15]. In the acidic pH range, the overall charge on the AC surface is positive and this results in repulsion forces between the adsorbent and the metal ions. This also explains the low uptake of the metals in the acidic pH range [21]. An increase in pH increases the negative charge on the surface due to the deprotonation of oxygen-containing functional groups and this leads to electrostatic attractions between the metal ions and the negatively charged sites [24], [31]. The adsorption capacity of the AC adsorbent is thus increased [38].

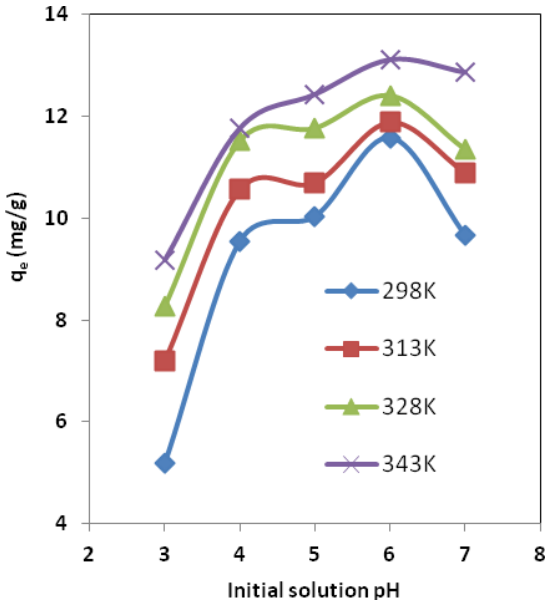

Fig. 5 Adsorption profile of Ni (II) by modified AC at different solution pH and temperature

An increase in temperature had a positive effect on the uptake of Ni(II) and Co(II) onto the oxalate-modified AC. For instance, for Ni(II) adsorption at an optimum pH of 6, an increase in temperature from 298-343K resulted in an increase in uptake from 11.57-13.12 mg/g.

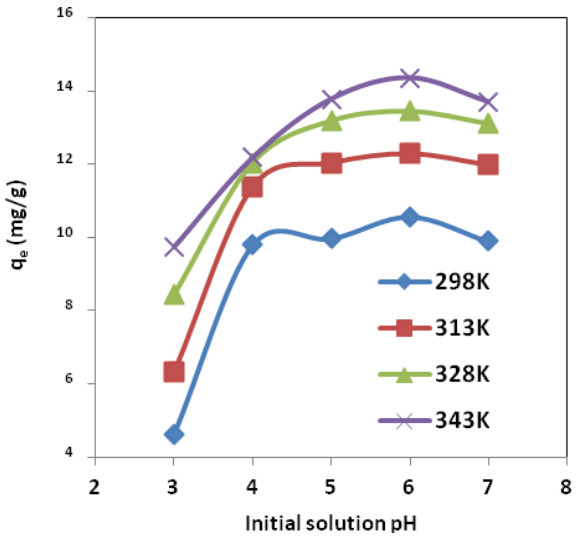

Fig. 6 Adsorption profile of Co(II) by modified AC at different solution pH and temperature

The initial adsorption kinetics profiles for Ni(II) and Co(II) are illustrated in Fig. 7 and 8. The rate of uptake of the Ni (II) and Co (II) ions is rapid in the first 30 minutes. Initially there is little competition for the metal ions for the adsorption sites because the available surface area is very large. Competition of metal ions for the remaining available adsorption sites increases as the surface coverage of the adsorbents increases. This slows down the rate of uptake of the ions [34], [42]. This was also observed by [1] when they adsorbed Cr(VI) using activated carbon prepared from *Tamarind wood* activated with zinc chloride. They attributed their observation to the increased concentration gradient that exists between the adsorbate in solution and adsorbate in adsorbent in the initial stage of adsorption.

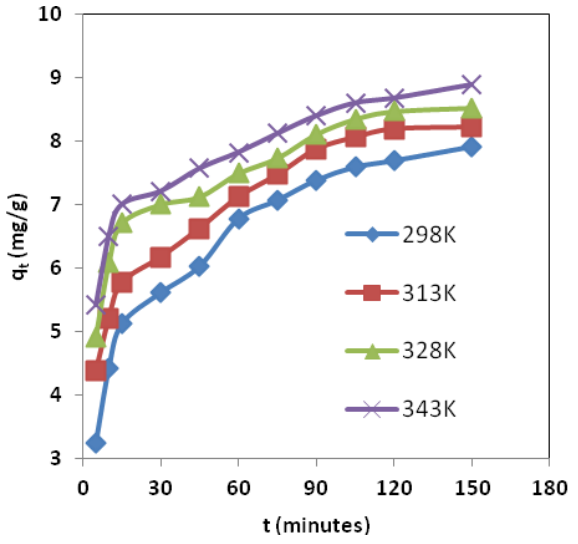

Fig. 7 Initial adsorption kinetics profiles for Ni(II) at different solution temperatures using oxalate-modified AC

Temperature had a significant effect on the rate of adsorption of Ni (II) and Co (II) onto the oxalate-modified AC. For instance, after an adsorption period of 30 minutes as shown in Fig. 8 below, the increase in temperature from 298-343K resulted in an increase in the uptake of cobalt from 5.62-7.62mg/g.

The pseudo-first-order and pseudo-second-order models were used to analyze the adsorption kinetics data. The first order kinetic processes signify reversible interactions with an equilibrium being established between liquid and solid phases. The pseudo-first-order kinetic model is given in differential form as [24]:

$$\frac{dq_t}{dt} = k_1(q_e - q_t) \quad (6)$$

Where $k_1(min^{-1})$ is the first-order rate constant of sorption, $q_e(mg/g)$ is the amount of metal ion adsorbed at equilibrium, $q_t(mg/g)$ is amount of metal ion on the surface of the sorbent at anytime.

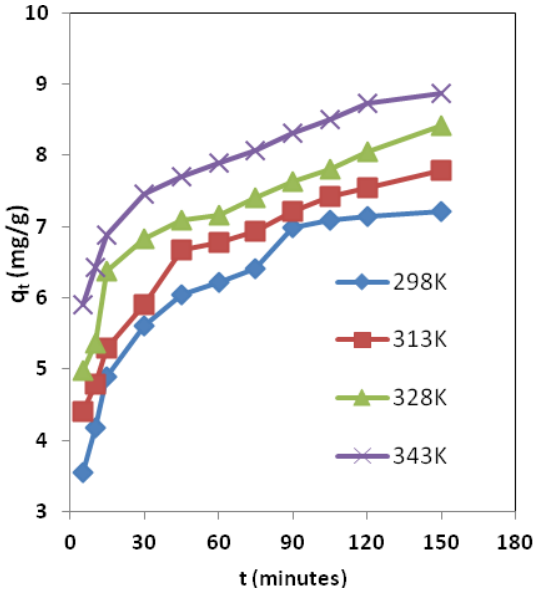

Fig. 8 Initial adsorption kinetics profiles for Co(II) at different solution temperatures using oxalate-modified AC

The linearized form of the pseudo-first-order kinetic model which is obtained by integrating (6) subject to the boundary conditions (t=0, q_t=0 and t=t, q_t=q_t) is expressed as [29]:

$$\log(q_e - q_t) = \log(q_e) - \frac{k_1}{2.303}t \quad (7)$$

The values of k_1 and q_e can be obtained from the slope and intercept of the straight-line plots of $\log(q_e - q_t)$ against t. To test the validity of (7) experimentally determined q_e values are compared to those obtained from the plots of $\log(q_e - q_t)$ vs. t. If this test is not valid, then higher order kinetic models are to be tested with respect to the experimental results [12].

The pseudo-second order model is given in differential form as [3]:

$$\frac{dq_t}{dt} = k_2(q_e - q_t)^2 \quad (8)$$

Where $k_2(g/mg\ min)$ is the second order rate constant of sorption

Upon separation of variables and integration of (8) subject to the boundary conditions (qt=0 at t=0 and qt=qtat t=t), a linear form is obtained and expressed as follows [30]:

$$\frac{t}{q_t} = \frac{1}{k_2(q_e)^2} + \frac{1}{qe}t \quad (9)$$

The constants k_2 and q_e can be calculated from the intercept and slope of straight line plots of t/q_t against t. k_2 depends on applied operating conditions such as the initial metal concentration in bulk solution, pH of the solution, temperature and agitation rate.

To make a meaningful comparison between the two models, two parameters were compared to decide on the model that best describes the kinetics of the adsorption process. The parameters were the correlation coefficients (R^2) and the normalized standard deviation, $\Delta q(\%)$ which is given as:

$$\Delta q(\%) = 100\sqrt{\frac{\sum[(q_{exp} - q_{cal})/q_{exp}]^2}{N-1}} \quad (10)$$

Where q_{exp} and q_{cal} are the experimental and calculated amount of Ni(II) and Co(II) adsorbed on AC adsorbents and N is the number of measurements made. The adsorption kinetics constants, correlation coefficients and the normalized standard deviation percentages are given in Table I.

TABLE I
KINETIC PARAMETERS FOR NI (II) AND CO (II) ADSORPTION ONTO OXALATE-MODIFIED AC

Metal	T (K)	$q_{e,exp}$ (mg/g)	Pseudo-first order rate equation				Pseudo-second order rate equation			
			k_1 (min^{-1})	q_1 (mg/g)	R^2	Δq (%)	k_2 (g mg^{-1} min^{-1})	q_2 (mg/g)	R^2	Δq (%)
Ni(II)	298	9.92	8.06×10^{-3}	5.65	0.92	43.00	8.58×10^{-3}	8.65	0.99	12.80
	313	10.62	5.99×10^{-3}	5.35	0.91	49.66	1.06×10^{-2}	8.84	0.99	16.74
	328	11.14	4.84×10^{-3}	5.19	0.92	53.40	1.31×10^{-2}	8.94	0.99	19.71
	343	11.9	3.92×10^{-3}	5.54	0.91	53.40	1.45×10^{-2}	9.07	0.99	23.81
Co(II)	298	9.03	7.37×10^{-3}	5.50	0.93	39.04	1.21×10^{-2}	7.76	0.99	14.09
	313	9.84	4.61×10^{-3}	5.53	0.90	43.78	1.31×10^{-2}	8.16	0.99	17.04
	328	10.63	4.38×10^{-3}	5.39	0.91	49.29	1.41×10^{-2}	8.66	0.99	18.55
	343	11.32	3.92×10^{-3}	5.33	0.92	52.93	1.63×10^{-2}	9.18	0.99	18.88

After analysis of the kinetics data, higher correlation coefficients (>0.99) were obtained from the plot of the second-order-kinetics model. The normalized standard deviation percentages (Δq) were also lower than those obtained from the first-order-kinetics model. The conformity of the experimental data to the second-order-kinetic model suggests that the adsorption of Ni (II) and Co (II) onto modified AC is chemical in nature [2], [31]. Fig. 9 and 10 illustrate the fitting of the kinetic data to the pseudo-second-order model for Ni(II) and Co(II), respectively.

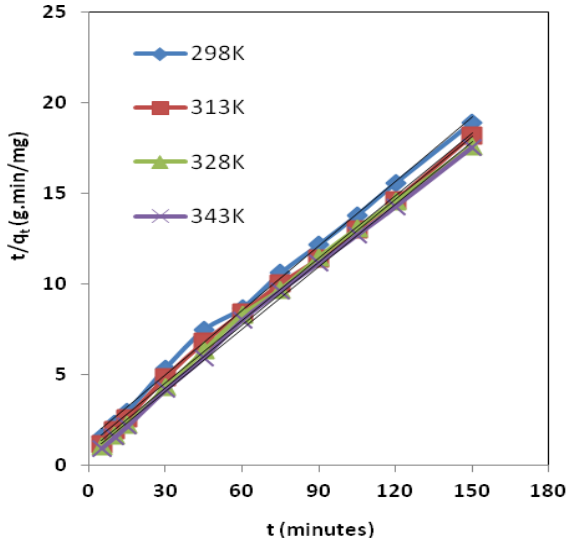

Fig. 9 The fitting of kinetics data to pseudo-second-order model for Ni(II) using oxalate-modified AC

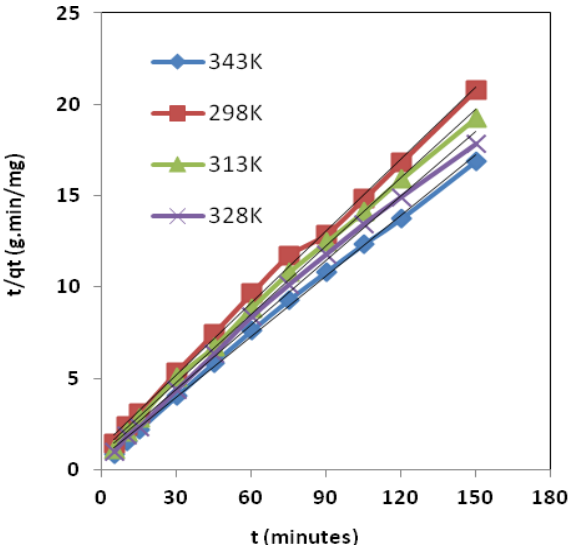

Fig. 10 The fitting of kinetics data to pseudo-second-order model for Co(II) using oxalate-modified ACs

An increase in the initial metal concentration of the solution from 30-150mg/L led to an increase in the uptake of the metal on the adsorbent, as shown in Fig. 11 and 12. For Co(II) adsorption onto the oxalate-modified AC at 298K, as shown in Fig. 11, the increase in metal concentration in the range studied resulted in an increase in uptake from 10.57-34.64mg/g. The driving force, which is the difference between the bulk phase and adsorbent phase concentrations, increases as the initial metal concentration is increased. This results in an increase in the uptake of the metal ions [43]. An increase in temperature resulted in an increase in the equilibrium uptake of the metals. The uptake of Ni(II), as shown in Fig. 12, increased from 37.14 to 44.87mg/g as the temperature was raised from 298 to 343K with the initial metal concentration fixed at 150mg/L. The increase in adsorption sites generated by the breaking of some internal bonds near the edge of the active sites of the adsorbent could be used to explain the increase in the uptake of the metals with an increase in temperature [1].

The qualitative information on the nature of solute-surface interaction and the relationship between the solute in solution and the extent of accumulation onto the adsorbent surface at a constant temperature can be described by an isotherm model [24]. The Langmuir and Freundlich isotherm models are employed to fit the equilibrium data from this work.

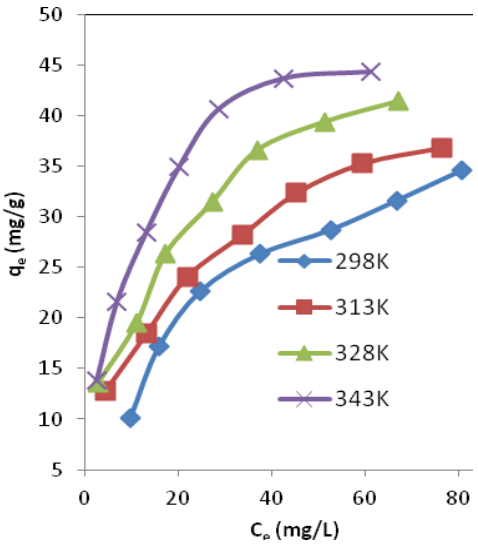

Fig. 11 Plot of equilibrium adsorption (q_e) of Co(II) versus equilibrium concentration (C_e) in solution. Temperature range 298 – 343 K. (Oxalate-modified AC)

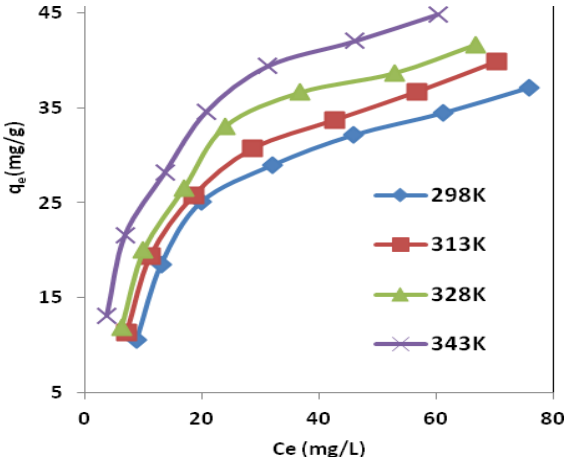

Fig. 12 Plot of equilibrium adsorption (q_e) of Ni(II) versus equilibrium concentration (C_e) in solution. Temperature range 298 – 343 K. (Oxalate-modified AC)

The Langmuir model can be expressed mathematically as follows [1]:

$$q_e = \frac{Q_m b C_e}{1 + b C_e} \quad (11)$$

Where q_e is the amount of metal ion adsorbed per weight of the adsorbent at equilibrium (mg/g), Q_m is the monolayer adsorption capacity (mg/g) and b is the Langmuir constant (L/g). This equation can be linearized to yield [9]:

$$\frac{C_e}{q_e} = \frac{1}{Q_m b} + \frac{C_e}{Q_m} \quad (12)$$

If the equilibrium data conforms to a Langmuir model, a plot of C_e/q_e vs C_e yields a straight line and the monolayer adsorption capacity (Q_m) and the Langmuir constant (b) can be calculated from the slope and intercept of the line, respectively.

The Freundlich isotherm is expressed mathematically as [2]:

$$q_e = K_f(C_e)^{1/n} \quad (13)$$

Where K_f and n are the equilibrium constants representing adsorption capacity and adsorption intensity, respectively. This equation can also be linearized to yield [6].

$$\log q_e = \log K_f + \frac{1}{n}\log C_e \quad (14)$$

A plot of $\log q_e$ vs $\log C_e$ yields a straight line if the data conforms to the Freundlich isotherm and the adsorption capacity and adsorption intensity constants can be calculated from the intercept and slope of the straight line, respectively

Fig. 13 and 14 show the fitting of the equilibrium data for Ni(II) and Co(II) onto the oxalate-modified AC adsorbent to the Langmuir isotherm model at different temperatures. The constants for the two isotherm models are summarized in Table II. From the plots and the correlation coefficients it is evident that the adsorption of Ni(II) and Co(II) conforms to the Langmuir isotherm model in the entire temperature range tested. This suggests that adsorption occurs on a homogeneous surface by monolayer adsorption without any interaction between adsorbed ions [7]. The values of n calculated from the Freundlich isotherm in Table II indicated that the adsorption process is favorable as n values of between 1 and 10 signifies efficient adsorption [28], [16].

The adsorption capacities for the metals ions studied differ because of their size, degree of hydration and the value of the binding constant with the adsorbent [25]. The endothermic nature of the adsorption process is further substantiated by the increase in equilibrium sorption uptake as well as the energy of adsorption (b) in Table II. A comparison of equilibrium capacities of Ni(II) and Co(II) onto oxalate-modified carbon to those reported in the literature is shown in Table III.

TABLE II
LANGMUIR AND FREUNDLICH CONSTANTS FOR THE ADSORPTION OF NI(II) AND CO(II) ONTO OXALATE-MODIFIED AC

Metal	Temperature (K)	Langmuir constants			Freundlich constants		
		Q_m (mg/g)	b (L/g)	R^2	K_f (mg/g)	n	R^2
Co(II)	298	45.25	3.69×10^{-2}	0.993	4.02	1.99	0.956
	313	46.30	5.08×10^{-2}	0.998	5.48	2.18	0.979
	328	50.25	6.86×10^{-2}	0.991	7.53	2.37	0.985
	343	50.76	1.23×10^{-1}	0.995	10.65	2.67	0.976
Ni(II)	298	46.08	5.24×10^{-2}	0.997	5.43	2.16	0.946
	313	49.50	5.46×10^{-2}	0.997	5.80	2.12	0.949
	328	51.02	6.58×10^{-2}	0.997	6.62	2.16	0.944
	343	52.63	9.13×10^{-2}	0.999	8.68	2.35	0.949

TABLE III
A COMPARISON OF EQUILIBRIUM CAPACITIES OF NI(II) AND CO(II) ONTO OXALATE-MODIFIED CARBON TO THOSE REPORTED IN THE LITERATURE

Adsorbent	Adsorbate	Maximum uptake (mg/g)	Reference
Esterified coir pith	Co(II)	34.13	[28]
Aminophosphonate chelating resin	Co(II)	8.01	[6]
Coir pith	Co(II)	12.82	[29]
	Ni(II)	15.95	
Black carrot residues	Co(II)	5.35	[13]
	Ni(II)	5.75	
Surface imprinted silica gel	Ni(II)	12.61	[14]
Na-Attapulgite	Ni(II)	5.28	[42]
Activated carbon cloths	Ni(II)	8.85	[10]
Amberlite IR-120 synthetic resin	Ni(II)	11.15	[7]
Oxalate modified activated carbon	Ni(II)	52.63	This work
	Co(II)	50.76	

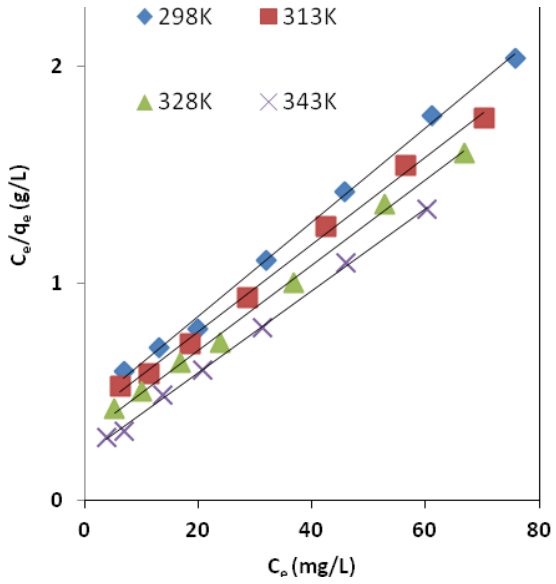

Fig. 13 A fit of Ni(II) equilibrium adsorption data to Langmuir Isotherms at different temperature using oxalate-modified AC

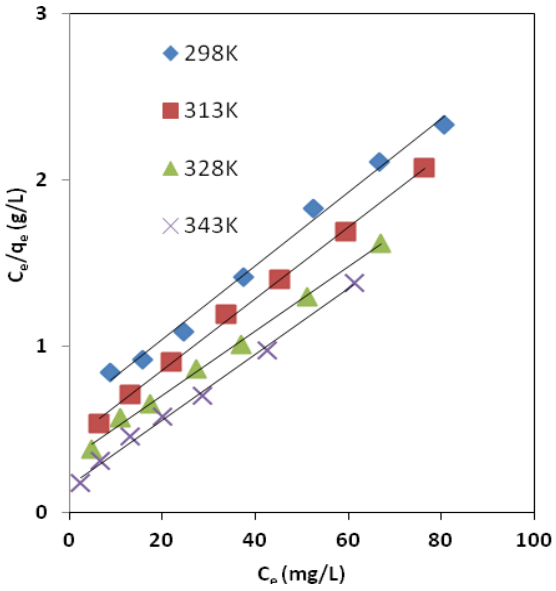

Fig. 14 A fit of Co(II) equilibrium adsorption data to Langmuir Isotherms at different temperature using oxalate-modified AC

Fig. 15 and 16 represent the removal efficiency as a function of adsorbent dose for Ni(II) and Co(II), respectively. An increase in adsorbent dose led to an increase in the removal efficiency of Ni(II) and Co(II) removal by the oxalate-modified AC adsorbent. At an optimum pH of 6 and temperature of 298K, an increase in adsorbent dose from 1 to 5g/L resulted in an increase in removal efficiency from 64.93 to 92.90% and 60.03 to 81.80% for Co(II) and Ni(II), respectively. When the adsorbent dose is increased there is an increase in the surface area and functional groups for complexation with metal ions. This increases the removal efficiency of the metal ions by the oxalate-modified AC

adsorbent [22], [16]. A similar trend was observed by [37] when they removed Cr (VI) from aqueous solutions using Alligator weed.

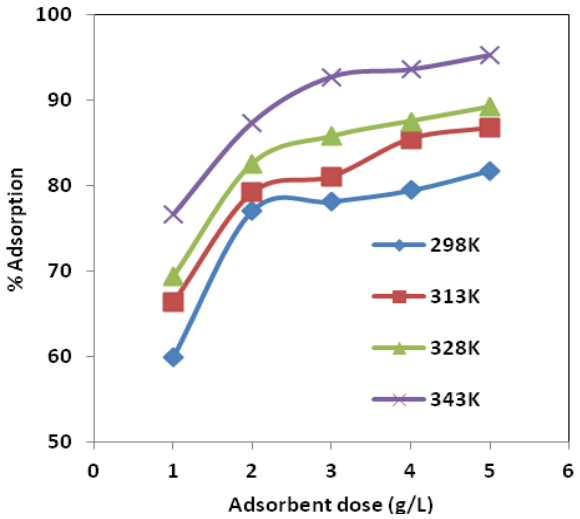

Fig. 15 Effect of adsorbent dose on Ni(II) adsorption onto oxalate-modified AC

The differences in removal efficiencies at various temperatures showed that temperature had an effect on the adsorption of Ni (II) and Co (II) ions. An increase in temperature led to an increase in the removal efficiencies of the metal ions. For instance, at an optimum pH of 6 and adsorbent dose of 3g/L, an increase in temperature from 298-343K resulted in an increase in the removal efficiency from 81.20-96.57% and 78.20-92.77% for Co(II) and Ni(II), respectively.

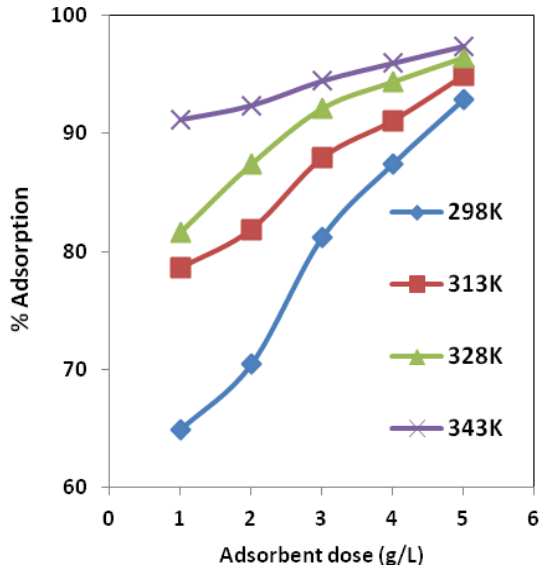

Fig. 16 Effect of adsorbent dose on Co(II) adsorption onto oxalate-modified AC

C. Simulations Results

The optimized geometry of the AC-oxalate structure when the AC is functionalized with a carboxylic acid group is shown in Fig. 17. The distances between the oxalate centre of mass and the carboxylic acid H1 (see Fig. 17 for labels), O1, C1 and O2 are 2.31, 3.25, 4.24 and 5.36 Å, respectively. It is therefore clear that the doubly negatively charged oxalate is attracted to the OH part of the carboxylic acid group, and not the O2, which has a negative charge of -0.45 in the COMPASS force field (H1 has a +0.41 charge and O1 a -0.455 charge).

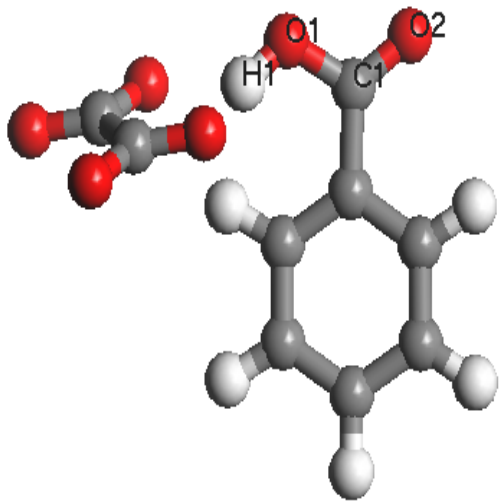

Fig. 17 Minimum energy structure of the AC-oxalate structure when the AC is functionalized with a carboxylic

The binding energy between the AC functionalized with the carboxylic acid and the oxalate is -34.79 kcal mol^{-1}. This strong bonding is accompanied by a rather large change in the structure of the AC compared to when it is isolated. These changes are mainly seen for the bond angles and torsions, and not for the bond lengths. For example, the C-C and C-O bonds in the oxalate differ by less than $8x10^{-3}$ and $4x10^{-3}$Å, respectively, and the carboxylic O1H1, C1O1, C1O2 bonds differ by less than $3x10^{-2}$, $8x10^{-3}$ and $2x10^{-3}$Å, respectively. The oxalate OCO angles differ by ≈1°, the carboxylic H1O1C1 and O1C1O2 angles differ by ≈8 and 28°, respectively, and the H1O1C1O2 torsion by ≈7.5°.

The AC-oxalate binding energies for all of the ACs studied here are listed in Table IV. It is evident that the binding to the carboxylic acid is strongest, followed by the ester, ketone and the ether functionalized ACs. The non-functionalized AC has a very weak bond, which indicates that the presence of functional groups on the AC surface is critical for adsorption of the oxalate ions.

TABLE IV
AC-OXALATE BINDING ENERGIES (KCAL MOL^{-1}) FOR THE FUNCTIONALIZED AND NON-FUNCTIONALIZED ACS

Functional group	E_{bind}
Carboxylic acid	-34.79
ester	-28.31
ketone	-24.60
ether	-11.62
no functional group	-4.99

The minimum energy structures for all of the AC-oxalate complexes are shown in Fig. 18. The distance between the oxalate centre of mass and the ester O1 is 12.25 Å. Similarly, the distance between the oxalate centre of mass and the ketone O1 atom is 12.35 Å. These separations differ significantly from the distance between the oxalate and ether O1 atom, which is 4.64 Å and the distance between the oxalate and the carboxylic acid group discussed above. In fact, as can be seen from Fig. 18 the oxalate is located on the side of the benzene ring that is furthest away from the ester and ketone functional groups, while it is located on the same side as the ether group. This is probably due to the fact that the O1 on the ester and ketone groups have large negative charges (-0.45) which repels the oxalate ion. Nevertheless, it is important to realize that the presence of the ester and ketone groups have a significant effect on the binding energy, which is far larger when these functional groups are present than when the benzene ring is not functionalized. In addition to this, geometry optimization was used to obtain AC-oxalate local minimum energy structures for the ester and ketone groups, where the oxalate was on the same side of the benzene ring as the functional group. The binding energies for these structures are -8.56 and -16.33 kcal mol^{-1}, respectively, which are weaker than for the structures shown in Fig. 18 (which have -28.31 and -24.60 kcal mol^{-1}, respectively).

The separation between the oxalate and the benzene centre of mass for the non-functionalized structure shown in Fig. 18d is 5.07 Å. In the non-functionalized AC–oxalate structure the oxalate lies to the side of the benzene ring. This is because the negatively charged oxalate is attracted to the hydrogen atoms (which have a charge of +0.13 in the COMPASS force field) and can be located near to these hydrogen atoms when adopting the structure shown in the figure.

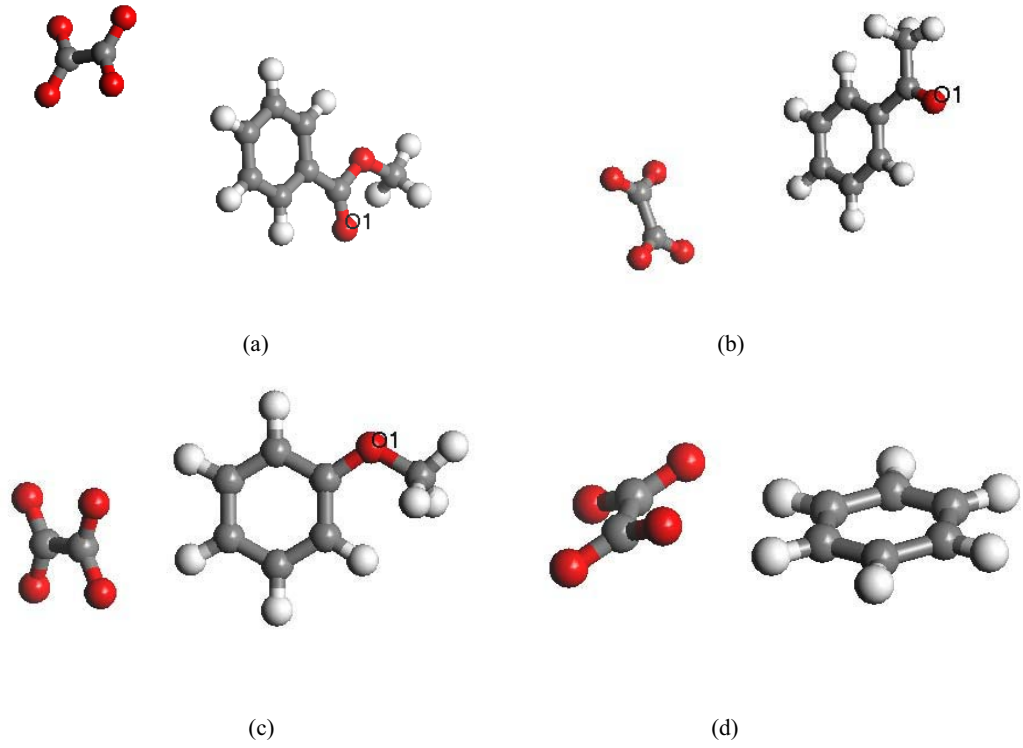

Fig. 18 Same as Fig. 17 but when the AC is functionalized with ester (a), ketone (b) and ether (c) functional groups. The structure in (d) is when there is no functional group

Since the carboxylic-acid functionalized AC showed the largest binding energy, it was used to study the effects of the addition of water on the system. Fig. 19 shows the minimum energy structure when six water molecules are added to the AC-oxalate system and when the AC is modified with a carboxylic acid group. It is clear that the water molecules are most strongly attracted to the oxalate ion, which is expected since the negatively charged ion attracts the positively charged hydrogen atoms of the water molecules (+0.41 in the COMPASS force field). Complete hydration of the oxalate ion is achieved with five water molecules, and the sixth water molecule does not strongly bind to the AC-oxalate complex (the water molecule that is furthest to the right in Fig. 19 is hydrogen bonded to two water molecules and not to the complex). What is of importance to the present study is that hydration of the oxalate ion does not cause it to desorb from the carboxylic acid functionalized AC, and hence this complex is stable in water medium.

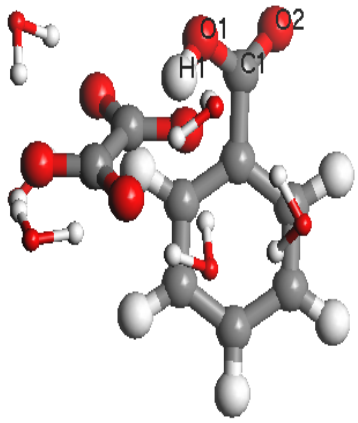

Fig. 19 Same as Fig. 17 but in the presence of six water molecules

It is clear from Fig. 19 that the oxalate is attracted to the OH part of the carboxylic acid, as was the case in the absence of water (see Fig. 17). A major difference caused by the hydration is that the oxalate has rotated approximately 90°, so that oxalate oxygen atoms that share a common carbon atom are now closest to the H1 atom. Presumably this occurs to enhance the hydration of the oxalate ion. However, hydration does not significantly change the intermolecular distance between the oxalate ion and the carboxylic group. In the presence of the water molecules the distances between the oxalate centre of mass and the carboxylic acid H1, O1, C1 and O2 are 2.65, 3.61, 4.52 and 5.66 Å, respectively. These are similar to the values of 2.31, 3.25, 4.24 and 5.36 Å, discussed above when no water is present.

In summary, the calculations show that oxygen containing functional groups play a significant role in the adsorption of oxalate ions onto AC surfaces. AC-oxalate complexes that contain some of these functional groups are also expected to be stable in aqueous medium, and this was explicitly shown for the carboxylic acid group.

Preliminary results indicate that AC-oxalate complexes that contain carboxylic acid, ketone, and ether functional groups are also stable in acidic media. Similarly to the results discussed above for water, addition of H_3O^+ ions to the complexes does not lead to significant changes in their structures. The effect of adding up to two H_3O^+ ions in the calculations (which is far more acidic than experiments) is that water molecules that solvate the oxalate are replaced by the added H_3O^+ ions. This is expected since there is stronger bonding between the negative oxalate ion and the positive H_3O^+ ions that between the oxalate and the neutral water molecules.

These calculations are being extended to investigate the binding of oxalate ions to AC surfaces at a variety of pH values, which is also relevant to the experiments. Under these conditions the surface is expected to be charged, which will affect the oxalate-AC structures and binding properties. Future studies will also focus on the binding of the metal ions to the oxalate-AC structures.

V. Conclusion

The modification of an activated carbon substrate with potassium oxalate and the removal of Co(II) and Ni(II) as model heavy metals by adsorption using the modified adsorbent was carried out in batch mode. A temperature of 343K and pH 11 were found to be the optimum conditions for anchoring oxalate molecules on the surface of native activated carbon. The FTIR absorbance at frequencies of 1199, 1102 and 1404cm^{-1} confirmed the presence of oxalate functional groups on the surface of modified activated carbon. The absorbance at these frequencies indicates the presence of C-O and COO^- functional groups. The maximum uptakes for cobalt and nickel adsorption were 50.76 and 52.63mg/g, respectively. Ni(II) and Co(II) equilibrium adsorption data fit the Langmuir isotherms very well in the temperature range 298-343K.

The experimental studies of oxalate ion adsorption on ACs were complemented by computational simulations on model oxalate-AC systems. It was seen that, under surface neutral conditions, the presence of carboxylic acid, ester, ketone and ether functional groups increases the magnitude of the adsorption energy of the oxalate ion to the AC surface. The oxalate ion adsorbed more strongly to the carboxylic acid group than to any of the other groups under these conditions, and that the presence of water does not destabilise these oxalate-AC complexes.

Co(II) and Ni(II) adsorption kinetics profile for the oxalate-modified carbon fit the pseudo-second-order kinetics model in the temperature range 298-343K. Temperature had a positive effect of the uptake of the metals onto the adsorbent and favourable adsorption was observed at higher temperatures. The oxalate-modified adsorbent cannot be used for the selective separation of nickel from cobalt but it has the potential to be applied in the selective separation of metal ions from negatively charged species such as $PdCl_6^{2-}$ or $PtCl_6^{2-}$. Ionic and covalent bonding of metal ions with anionic species of oxalates on AC surface is responsible for their removal from solution. The rejection of negatively charged chloro-

complexes would come as a result of repulsive forces that exist between them and the oxalate anions.

ACKNOWLEDGMENT

The authors acknowledge the financial support received from Xstrata through a skills capacity development and R&D grant awarded to TUT during the period 2008 and 2010.They are also grateful to The Swedish International Development Cooperation Agency for financial support. The calculations were performed using the Materials Studio program from Accelrys Software Inc.

REFERENCES

[1] Acharya, J., Sahu, J. N., Sahoo, B. K., Mohanty, C. R. & MEIKAP, B. C. (2009) Removal of chromium(VI) from wastewater by activated carbon developed from Tamarind wood activated with zinc chloride. Chemical Engineering Journal, 150, 25-39

[2] Ahn, C. K., Park, D., Woo, S. H. &Park, J. M. (2009) Removal of cationic heavy metal from aqueous solution by activated carbon impregnated with anionic surfactants. Journal of Hazardous Materials, 164, 1130-1136.

[3] Allen, S. J., Gan, Q., Matthews, R. &Johnson, P. A. (2005) Kinetic modeling of the adsorption of basic dyes by kudzu. Journal of Colloid and Interface Science, 286, 101-109.

[4] Bunte S. W., Sun H. (2000) Molecular modeling of energetic materials: The parameterization and validation of nitrate esters in the COMPASS force field, J. of Phys. Chem. B2000, 104, 2477-2489.

[5] Chingombe, P., Saha, B. & Wakeman, R.J. (2005) Surface modification and characterisation of a coal-based activated carbon. Carbon, 43, 3132-3143.

[6] Deepatana, A. &Valix, M. (2006) Recovery of nickel and cobalt from organic acid complexes: Adsorption mechanisms of metal-organic complexes onto aminophosphonate chelating resin. Journal of Hazardous Materials, B137, 925-933.

[7] Demirbas, A., Pehlivan, E., Gode, F., Altun, T. &Arslan, G. (2005) Adsorption of Cu(II), Zn(II), Ni(II), Pb(II), and Cd(II) from aqueous solution on Amberlite IR-120 resin. Journal of Colloid and Interface Science, 282, 20-25.

[8] Erdogan, S., Önal, Y., Akmil , C., BilmezErdemoglu, S., Sarıcı-Özdemir, Ç. & İcduygy, G. (2005) Optimization of nickel adsorption from aqueous solution by using activated carbon prepared from waste apricot by chemical activation. Applied Surface Science, 252, 1324-1331.

[9] Fan, Q., Shao, D., Lu, Y., Wu, W. &Wang, X. (2009) Effect of pH, ionic strength, temperature and humic substances on the sorption of Ni(II) to Na-attapulgite. Chemical Engineering Journal, 150, 188-195.

[10] Faur-Brauquet, C., Reddad, Z., Kadirvelu, K. & LeCloirec, P. (2002) Modelling the adsorption of metal ions (Cu2+, Ni2+, Pb2+) onto ACCs using surface complexation models. Applied Surface Science, 196, 356-365.

[11] Freid J. R., Mark A. E., (Ed.) (2006) Computational Parameters Physical properties of polymers handbook, 2nd edition, Springer, Chapter 4, p-64.

[12] Gupta, S. S. & Bhattacharyya, K. G. (2011) Kinetics of adsorption of metal ions on inorganic materials: A review. Advances in Colloid and Interface Science, 162, 39-58.

[13] Guzel, F., Yakut, H. & Topal, G. (2008) Determination of kinetic and equilibrium parameters of the batch adsorption of Mn(II), Co(II), Ni(II) and Cu(II) from aqueous solution by black carrot (Daucus carota L.) residues. Journal of Hazardous Materials, 153, 1275-1287.

[14] Jiang, N., Chang, X., Zheng, H., He, Q. & Hu, Z. (2006) Selective solid-phase extraction of nickel (II) using a surface-imprinted silica gel sorbent. Analytica Chimica Acta, 577, 225-231.

[15] Kadirvelu K., Senthilkumar P., Thamaiselvi K. &Subburam V. (2002) Activated carbon prepared from biomass as adsorbent: elimination of Ni (II) from aqueous solution. Bioresource Technology, 81, 87-90.

[16] Kadirvelu K., Thamaraiselvi K. &Namasivayam C. (2001) Adsorption of nickel (II) from aqueous solution onto activated carbon prepared from coirpith. Separation and Purification Technology, 24, 497-505.

[17] Kasaini, H., G. Masahiro and F. Shintaro., (2000) Selective separation of Pd (II), Rh (III), and Ru (III) ions from a mixed chloride solution using activated carbon pellets. Separation Science and Technology, 35(9), 1307-1327.

[18] Kasaini, H., Masahiro, G., Shin taro, F., (2001) Adsorption performance of activated carbon pellets immobilized with organo phosphorus extractants and an amine; a case study for the separation of Pt (IV), Pd (II), and Rh (III) ions in chloride media. Separation Science and Technology, 36(13), 2845-2861.

[19] Kasaini, H., Everson, R. (2003) Equilibrium and Kinetics of Palladium Adsorption on Carbon Surfaces. In: Abstracts of the XXII International Mineral Processing Congress. Cape Town, South Africa, 29 September – 3 October, p182.

[20] Kobya, M., Demirbas, E., Senturk, E. &Ince, M. (2005) Adsorption of heavy metal ions from aqueous solutions by activated carbon prepared from apricot stone. Bioresource Technology, 96, 1518-1521.

[21] Krishnan, K. A. &Anirudhan, T. S. (2008) Kinetic and equilibrium modelling of cobalt(II) adsorption onto bagasse pith sulphurised activated carbon. Chemical Engineering Journal, 137, 257-264.

[22] Lata, H., Garg, V. K. &Gupta, R. K. (2008) Sequestration of nickel from aqueous solution onto activated carbon prepared from Parthenium hysterphorus L. Journal of Hazardous Materials, 157, 503-509.

[23] Leach A. (2001) Molecular modelling: principles and applications, 2nd ed. (Prentice Hall, London) pps 262-273.

[24] Li, K. & Wang, X. (2009) Adsorptive removal of Pb(II) by activated carbon prepared from Spartina alterniflora: Equilibrium, kinetics and thermodynamics. Bioresource Technology, 100, 2810-2815.

[25] Li, Z., Chang, X., Hu, Z., Huang, X., Zou, X., Wu, Q. & Nie, R. (2009) Zincon-modified activated carbon for solid-phase extraction and preconcentration of trace lead and chromium from environmental samples. Journal of Hazardous Materials 166, 133-137.

[26] Mphahlele, R.C.J., Bolton, K. & Kasaini, H. (2010) Computational studies of binding energies and structures of methylamine on functionalized activated carbon surfaces. World Academy of Science, Engineering and Technology, 47.

[27] Mugisidi, D., Ranaldo, A., Soedarsono, J. W. & Hikam, M. (2007) Modification of activated carbon using sodium acetate and its regeneration using sodium hydroxide for the adsorption of copper from aqueous solution. Carbon, 45, 1081-1084.

[28] Parab, H., Joshi, S., Shenoy, N., Lali, A., Sarma, U. S. & Sudersanam, M. (2008) Esterified coir pith as an adsorbent for the removal of Co(II) from aqueous solution. Bioresource Technology, 99, 2083-2086.

[29] Parab, H., Joshi, S., Shenoy, N., Lali, A., Sarma, U. S. &Sudersanan, M. (2006) Determination of kinetic and equilibrium parameters of the batch adsorption of Co(II), Cr(II) and Ni(II) onto coir pith. Process Biochemistry, 41, 609-615.

[30] Plazinki, W., Rudzinki, W. & Plazinska, A. (2009) Theoretical models of sorption kinetics including a surface reaction mechanism: A review. Advances in Colloid and Interface Science, 152, 2-13.

[31] Popuri, S. R., Vijaya, Y., Boddu, V. M. &Abburi, K. (2009) Adsorptive removal of copper and nickel ions from water using chitosan coated PVC beads. Bioresource Technology, 100, 194-199.

[32] Sahu, K.K., Ag Agarwal, A. & Pandey, D.B. (2005) Nickel recovery from spent nickel catalyst.Waste Management & Research, 23: 148

[33] Saygideger, S., Gulnaz, O., Istifli, E. S. &Yucel, N. (2005) Adsorption of Cd(II), Cu(II) and Ni(II) ions by Lemna minor L.: Effect of physicochemical environment. Journal of Hazardous Materials, B126, 96-104.

[34] Sharma, N., Kaur, K. &Kaur, S. (2009) Kinetic and equilibrium studies on the removal of Cd2+ ions from water using polyacrylamide grafted rice (Oryza sativa) husk and (Tectona grandis) saw dust. Journal of Hazardous Materials, 163, 1338-1344.

[35] Sun, H. (1998) COMPASS: An ab initio force-field optimized for condensed-phase applications overview with details on alkane and benzene compounds. Journal of Physical Chemistry, B 102, 7338-7364.

[36] Sun, L. & Qiu, K. (2012) Organic oxalate as leachant and precipitant for the recovery of valuable metals from spent lithium-ion batteries. Waste Management

[37] Wang, X. S., Tang, Y. P. & Tao, S. R. (2009) Kinetics, equilibrium and thermodynamic study on removal of Cr (VI) from aqueous solutions using low-cost adsorbent Alligator weed. Chemical Engineering Journal, 148, 217-225.

[38] Xin, H., Nai-Yun, G. &Qiao-Li, Z. (2007) Thermodynamics and kinetics of cadmium adsorption onto oxidized granular activated carbon. Journal of Environmental Sciences, 19, 1287-1292.

[39] Yin, C. Y., Aroua, M. K. &Daud, W. M. A. W. (2007) Impregnation of palm shell activated carbon with polyethyleneimine and its effects on Cd2+ adsorption. Colloids and Surfaces, 307, 128-136.
[40] Sengupta, B., Tamboli, A.C. & Sengupta, R. (2011) Synthesis of nickel oxalate particles in the confined internal droplets of W/O emulsions and in systems without space confinement. Chemical Engineering Journal, 169, 379–389
[41] Ghaedi, M., Ahmadi, F. & Shokrollahi, A. (2007) Simultaneous preconcentration and determination of copper, nickel, cobalt and lead ions content by flame atomic absorption spectrometry. Journal of Hazardous Materials, 142, 272-278.
[42] Gupta, S. S. & Bhattacharyya, K. G. (2006) Adsorption of Ni(II) on clays. Journal of Colloid and Interface Science, 295, 21-32.
[43] Benamor, M., Bouariche, Z., Belaid, T., Draa, M.T. (2008) Kinetic studies on cadmium ions by Amberlite XAD7 impregnated resins containing di(2-ethylhexyl) phosphoric acid as extractant. Separation and Purification Technology, 59, 74–84